

# Distinct Roles for Tsg101 and Hrs in Multivesicular Body Formation and Inward Vesiculation<sup>□</sup>

M. Razi and C. E. Futter

Institute of Ophthalmology, University College London, London EC1V 9EL, United Kingdom

Submitted November 16, 2005; Revised April 28, 2006; Accepted May 8, 2006

Monitoring Editor: Sandra Schmid

In mammalian cells, epidermal growth factor (EGF) stimulation promotes multivesicular body (MVB) formation and inward vesiculation within MVB. Annexin 1 is required for EGF-stimulated inward vesiculation but not MVB formation, demonstrating that MVB formation (the number of MVBs/unit cytoplasm) and inward vesiculation (the number of internal vesicles/MVB) are regulated by different mechanisms. Here, we show that EGF-stimulated MVB formation requires the tumor susceptibility gene, Tsg101, a component of the ESCRT (endosomal sorting complex required for transport) machinery. Depletion of Tsg101 potently inhibits EGF degradation and MVB formation and causes the vacuolar domains of the early endosome to tubulate. Although Tsg101 depletion inhibits MVB formation and alters the morphology of the early endosome in unstimulated cells, these effects are much greater after EGF stimulation. In contrast, depletion of hepatocyte growth factor receptor substrate (Hrs) only modestly inhibits EGF degradation, does not induce tubulation of the early endosome, and causes the generation of enlarged MVBs that retain the ability to fuse with the lysosome. Together, these results indicate that Tsg101 is required for the formation of stable vacuolar domains within the early endosome that develop into MVBs and Hrs is required for the accumulation of internal vesicles within MVBs and that both these processes are up-regulated by EGF stimulation.

## INTRODUCTION

Receptors destined for lysosomal degradation are sorted from those that are to be recycled to the plasma membrane in multivesicular endosomes/bodies (MVBs) (Katzmann *et al.*, 2002; Gruenberg and Stenmark, 2004). Recycling receptors such as transferrin receptor (TFR) remain on the limiting membrane of the MVB from where they are returned to the cell surface. Lysosomally directed receptors such as epidermal growth factor (EGF) receptors (EGFRs) are removed from the perimeter membrane and are sorted onto internal vesicles. When all the recycling proteins have been removed, MVBs fuse with lysosomes and the receptor and ligand are degraded (van Deurs *et al.*, 1995; Futter *et al.*, 1996; Mullock *et al.*, 1998).

Components of the core machinery required for the sorting of cargo within MVBs have been identified in yeast and include the endosomal sorting complex required for transport (ESCRT) protein complexes (ESCRT-0, -I, -II, and -III) that are thought to act sequentially in the selection of proteins for retention within MVBs (Katzmann *et al.*, 2001; Babst

*et al.*, 2002a, b; Babst, 2005). At least one homologue of all the ESCRT components identified in yeast have been found in mammalian cells, suggesting conservation of the core MVB sorting machinery. However, the role of the ESCRT proteins has not been fully characterized in mammalian cells. Existing models propose that the hepatocyte growth factor receptor substrate (Hrs) complex (ESCRT-0) concentrates ubiquitinated proteins destined for lysosomal degradation on the perimeter membrane of the early endosome (Raiborg *et al.*, 2002; Sachse *et al.*, 2002; Bilodeau *et al.*, 2003; Urbe *et al.*, 2003) and recruits ESCRT-I via direct interaction with the tumor susceptibility gene, Tsg101 (Bache *et al.*, 2003; Bilodeau *et al.*, 2003; Katzmann *et al.*, 2003; Lu *et al.*, 2003). Tsg101 is a component of ESCRT-I, interacts with ubiquitinated proteins (Bishop *et al.*, 2002), and is required for efficient degradation of EGF/EGFR (Babst *et al.*, 2000; Doyotte *et al.*, 2005).

ESCRT-mediated cargo selection is thought to be coupled to inward vesiculation within MVBs in a process involving disassembly of the ESCRT complexes by the ATPase vacuolar protein sorting (Vps)4. Overexpression of Hrs (Urbe *et al.*, 2003) or expression of dominant negative Vps4 (Sachse *et al.*, 2004) inhibit inward vesiculation within MVB. Inward vesiculation within MVBs has the same topology as viral budding. The demonstration that Tsg101 binds the late budding motif, PT(IP), of the human immunodeficiency virus (HIV) GAG protein (Garrus *et al.*, 2001; Martin-Serrano *et al.*, 2001; VerPlank *et al.*, 2001) and depletion of Tsg101 inhibits HIV budding (Garrus *et al.*, 2001) suggests that Tsg101 may have a direct role in the inward invagination process. Consistent with a structural role for ESCRT complexes in the endocytic pathway is the demonstration that deletion of components of ESCRT-I result in the formation of multilamellar ring-like structures in some yeast cells (Raymond *et al.*, 1992; Rieder *et al.*, 1996), which have been termed the class E compartment. Moreover, in a recent study, depletion

This article was published online ahead of print in *MBC in Press* (<http://www.molbiolcell.org/cgi/doi/10.1091/mbc.E05-11-1054>) on May 17, 2006.

<sup>□</sup> The online version of this article contains supplemental material at *MBC Online* (<http://www.molbiolcell.org>).

Address correspondence to: Clare Futter (c.futter@ucl.ac.uk).

Abbreviations used: EEA1, early endosome antigen 1; EGFR, epidermal growth factor receptor; ESCRT, endosomal sorting complex required for transport; Hrs, hepatocyte growth factor receptor substrate; MVB, multivesicular body; siRNA, small interfering RNA; TEM, transmission electron microscope; TF, transferrin; TFR, transferrin receptor; Tsg, tumor susceptibility gene; Vps, vacuolar protein sorting.

of Tsg101 in mammalian cells was shown to cause major changes in the morphology of the early endosome and to induce the formation of a multicisternal compartment reminiscent in structure of the class E compartment (Doyotte *et al.*, 2005). The morphology of these class E compartments in both yeast and mammalian cells suggests that ESCRT complexes may play structural roles in the endocytic pathway in addition to inward invagination. Indeed depletion of Tsg101 in mammalian cells was found to compromise multiple transport steps, including delivery to the lysosome and recycling to the cell surface and the *trans*-Golgi network (Doyotte *et al.*, 2005).

In this study, we have dissected the respective roles of Tsg101 and Hrs in structural events within the endocytic pathway, focusing on their role in the biogenesis of MVBs. In our previous quantitative studies, we have shown that the number of MVBs and the number of internal vesicles within them are separately regulated (White *et al.*, 2006). EGF stimulation promotes MVB formation (the number of MVBs/U cytoplasm) and inward vesiculation (the number of internal vesicles/MVB). In the absence of annexin 1, EGF-stimulated increase in MVB number is maintained, but the increase in internal vesicle number/MVB is abolished. Thus, annexin 1 is not required for EGF stimulated MVB formation, but it is a requirement for EGF-stimulated internal vesicle formation. Annexin 1 is not required for any part of MVB biogenesis in unstimulated cells and is not even expressed in yeast. ESCRT complexes are likely to be part of the core MVB machinery, but their roles in MVB biogenesis have not been clearly defined. Here, we use quantitative electron microscopic (EM) analysis to determine the roles of Tsg101 and Hrs in MVB formation and inward vesiculation.

## MATERIALS AND METHODS

### Reagents

Monoclonal antibody (mAb) to the extracellular domain of the EGF receptor (108) was a gift from J. Schlessinger (New York University Medical Center, New York, NY). Gold particles (10 nm; British Biocell International, Cardiff, South Glamorgan, United Kingdom) were stabilized with the mAb 108, according to standard procedures (DeMey, 1986). mAb to Hrs (ALX-804-382) was from Alexis Biochemicals (Lausen, Switzerland). Tsg101 mAb (ab83) was purchased from Genetex (San Antonio, TX). Goat anti-EGF receptor polyclonal antibody (1005-G) was from Santa Cruz Biotechnology (Santa Cruz, CA). Early endosome antigen (EEA)1 mAb (E41120-050) was purchased from BD Transduction Laboratories (Lexington, KY). Rab11 rabbit antibody (71-5300) was from Zymed Laboratories (South San Francisco, CA). Alexa-conjugated transferrin (TF) and EGF were from Invitrogen (Carlsbad, CA). Human EGF (E9644) and transferrin (T4132) were from Sigma-Aldrich (St. Louis, MO). Streptavidin-horseradish peroxidase (HRP) and biotinylated EGF were purchased from Invitrogen and were used to produce HRP-conjugated EGF by mixing 5  $\mu$ g of strep-HRP and 0.3  $\mu$ g of biotinylated EGF in 300  $\mu$ l of phosphate-buffered saline (PBS) overnight at 4°C.

Human (h)EGF receptor construct was a generous gift from Alexander Sorkin (University of Colorado, Denver, CO). The first small interfering RNAs (siRNAs) against Tsg101, Hrs, and control inverted (Inv) sequence were as described previously (Garrus *et al.*, 2001; Bache *et al.*, 2003) and from Qiagen-Xeragon (Germantown, MD). The second siRNAs against Tsg101 and Hrs were from Dharmacon RNA Technologies (Lafayette, CO), and RNA sequences for Tsg101 were sense, CCA GUC UUC UCU CGU CCU A dTdT and antisense, UAG GAC GAG AGA AGA CUG G dTdT; and for Hrs were sense, AGA GAC AAG UGG AGG UAA A dTdT and antisense, UUU ACC UCC ACU UGU CUC U dTdT.

### Cells and Transfections

Human epidermoid carcinoma cell line (A431) and human embryonic kidney (HEK) 293T cells were maintained in 10% DMEM. A431 cells were transfected by using either Oligofectamine (Invitrogen) as described previously (Garrus *et al.*, 2001) or by using the nucleofector (Amaxa Biosystems, Cologne, Germany) following the manufacturer's instructions.

For Hrs siRNA transfection, on day 1 A431 cells were nucleofected with the siRNA or the control inverted oligonucleotide (oligo) (1.5–2.5  $\mu$ g) using solution R and program T20. Forty-eight hours after the first nucleofection, cells were harvested and nucleofected for the second time. Transfection efficiency was analyzed 48 h after the second transfection by Western blotting.

HEK293T cells were transfected using the nucleofector following the manufacturer's instructions with some modifications. Briefly, on day 1 cells were cotransfected with the hEGF receptor cDNA (3  $\mu$ g) and either siRNA against Tsg101 or the control inverted oligo (1.5–2  $\mu$ g) using solution V and program T23. Forty-eight hours after the first nucleofection cells were harvested and nucleofected for the second time with the siRNA or the control oligo (Inv). Transfection efficiency was analyzed 48 h after the second transfection by Western blotting.

HEK293T cells were transfected using the nucleofector following the manufacturer's instructions with some modifications. Briefly, on day 1 cells were cotransfected with the hEGF receptor cDNA (3  $\mu$ g) and either siRNA against Tsg101 or the control inverted oligo (1.5–2  $\mu$ g) using solution V and program T23. Forty-eight hours after the first nucleofection cells were harvested and nucleofected for the second time with the siRNA or the control oligo (Inv). Transfection efficiency was analyzed 48 h after the second transfection by Western blotting.

### Western Blot

Growing cells were lysed in reducing sample buffer and separated on 10% SDS-PAGE gel and transferred onto nitrocellulose membrane. The membrane was blocked with blocking buffer (5% skimmed milk in PBS-Tween) for at least 20 min. The membranes were probed with the appropriate primary antibody for an hour. The antibody was labeled with an HRP-conjugated secondary antibody from Dako UK (Ely, Cambridgeshire, United Kingdom) and visualized with enhanced chemiluminescence (catalog no. 34080; Pierce Chemical (Rockford, IL) and Intelligent Dark Box II and Image Reader LAS-1000 software (Fujifilm, Tokyo, Japan). The blots were also probed for tubulin as a protein loading control.

### Confocal Microscopy

Cells were serum-starved for an hour and stimulated with Alexa 488-conjugated EGF for the specified length of time. The labeled EGF was chased using serum-free medium with or without unlabeled human EGF (1  $\mu$ g/ml). Cells (except for Hrs staining) were fixed in 4% paraformaldehyde containing 3% sucrose permeabilized by 0.5% Triton X-100 for 5 min and blocked with 1% bovine serum albumin (BSA) for at least 20 min. Cells were labeled with the primary antibody for an hour followed by incubation with an appropriate secondary antibody. For Hrs staining, cells were fixed with precooled (–20°C) methanol for 5 min at room temperature. The coverslips bearing cells were dried at room temperature for 8 min followed by overnight rehydration using PBS at 4°C and were then blocked with 10% serum for 30 min. Cells were labeled with the primary antibody in 5% serum for an hour followed by incubation with an appropriate secondary antibody.

The images were collected using a Leica TCS SP2 AOBS confocal system attached to a Leica DMIRE2 microscope. Images were acquired using 63 $\times$ /1.4 (variable numerical aperture [NA] APO) oil immersion objective and Leica confocal software. Image processing was done with Adobe Photoshop, version 7.0 (Adobe Systems, Mountain View, CA).

### Electron Microscopy

Cells were serum-starved for an hour and stimulated with either HRP-conjugated EGF, Alexa 488-conjugated EGF, or human EGF (Sigma-Aldrich) in the presence of 108 (anti-EGFR) gold for the specified length of time. Cells were fixed in 0.1 M cacodylate containing 2% paraformaldehyde and 2% glutaraldehyde. For correlative light and electron microscopy (EM), cells were first imaged with a 20 $\times$ /0.5NA phase objective on an Imposition Openlabs system with a Zeiss Axiovert 100M microscope and then processed for EM. For EM, HRP-EGF-stimulated cells were incubated with hydrogen peroxide and diaminobenzidine tetrahydrochloride (DAB) as described by Graham and Karnovsky (1966), and they were then embedded as described previously (Futter *et al.*, 2001), except cells which contained DAB product were not treated with tannic acid and the sections were not stained with lead citrate. Thin (70-nm) and thick (200-nm) sections were viewed in a JOEL1010 transmission electron microscope.

For quantitative analysis thin sections were examined. Random photos within the cells were taken, and vacuoles with a diameter of >200 nm containing one or more internal vesicles, whether they had EGFR or not, were analyzed. Vacuoles that contained multilamellar profiles, indicating that they were lysosomal, were excluded. Cytoplasmic area and MVB areas were measured using LaserPix software (Bio-Rad, Hercules, CA), and the number of MVBs and internal vesicles within the MVBs was counted. At least three separate experiments were performed for each treatment, and >2,000  $\mu$ m<sup>2</sup> of cytoplasm was examined in each case. More than 70 MVBs were examined for statistical analysis for each treatment.

### Iodinated EGF Degradation and Recycling

Cells were incubated with <sup>125</sup>I-EGF (~1 ng/ml; GE Healthcare, Little Chalfont, Buckinghamshire, United Kingdom) in binding medium (0.05% BSA in serum-free culture medium) for 10 min at 37°C. A431 cells were surface stripped using 0.1 M glycine, 0.9% NaCl, pH 3.0, at 4°C and washed with binding medium. Cells were incubated with fresh prewarmed binding medium with or without unlabeled EGF (1.5  $\mu$ g/ml). After each time point, the medium was collected and replaced by fresh medium for the subsequent time point. HEK293T cells were plated on poly-L-lysine (Sigma-Aldrich) [used at 0.01% wt/vol] to improve their attachment to the plate, and separate wells

were used for each time point. The collected media were trichloroacetic acid (TCA) (20%) precipitated at 4°C for 1 h. TCA-precipitable proteins were pelleted by centrifugation at  $14,000 \times g$  at 4°C, and supernatant was collected. Cells were lysed in 1% Triton X-100, and the radioactivity in the chase medium, the TCA supernatant, and cell lysates was counted to determine the percentage of EGF degradation and recycling.

For transferrin recycling, A431 cells were incubated with  $^{125}\text{I}$ -TF (0.3  $\mu\text{g}/\text{ml}$ ; PerkinElmer Life and Analytical Sciences, Boston, MA) for 30 min at 37°C.  $^{125}\text{I}$ -TF was washed, and cells were surface stripped and incubated in fresh prewarmed binding medium. After each time point, the medium was collected and replaced by fresh medium for the subsequent time point. Cells were lysed in 1% Triton X-100, and the amount of radioactivity in the chase medium and cell lysates was determined. The data presented excludes the stimulation period.

## RESULTS

### Tsg101 Depletion Inhibits EGF Degradation

siRNAs were used to deplete endogenous Tsg101 in A431 and HEK293T cells. Control cells were oligofected with an oligonucleotide consisting of a heterologous control RNA duplex of Inv sequence (Garrus *et al.*, 2001). In our hands, no commercially available Tsg101 antibody gave a specific signal by immunofluorescence, so we were unable to identify individual Tsg101-depleted cells, but Western blotting indicated >90% depletion within the population of siRNA-treated cells, whereas Tsg101 levels were unaffected by treatment with control oligonucleotides (Figure 1A).

To examine whether Tsg101-depleted cells are defective in EGF degradation, cells were stimulated with  $^{125}\text{I}$ -EGF for 10 min at 37°C and then washed and surface stripped on ice and incubated with fresh binding medium at 37°C. At subsequent time points, medium was collected and fresh medium was added. During 4-h chase, Tsg101-depleted A431 cells degraded significantly less internalized  $^{125}\text{I}$ -EGF (31%) compared with control cells (57%) (Figure 1B). Although the degradation of EGF was significantly reduced, subsequent experiments revealed that more complete knockdown of Tsg101 reduces the degradation of EGF even more (see following experiments and Figure 8B). Similar results were obtained from HEK293T cells. Some HEK293T cells were transiently transfected with human EGFR to facilitate the following of EGFR traffic by EM. The overall degradation of EGF was lower in EGF receptor-overexpressing HEK293T cells, presumably because of saturation of the lysosomal targeting machinery. However, EGF degradation was reduced by Tsg101 depletion regardless of the levels of EGF receptor expression (Figure 1B).

### Tsg101 Depletion Causes Major Morphological Changes to EGFR-containing Compartments

To determine the effects of Tsg101 depletion on EGFR-containing endosomes, cells were incubated with anti-EGF receptor gold and EGF at 37°C (Figure 2). EGFR-gold could be found in vacuoles with the morphological appearance of MVBs that tended to be larger in siRNA-treated cells and had fewer internal vesicles, although internal vesicles could still form (Figure 2, A and B). MVBs containing very few as well as those containing many internal vesicles could be found within the same siRNA-treated cells, indicating that the presence of internal vesicles was not simply because that cell had failed to take up the siRNA.

Although EGFR could be found in vacuoles in siRNA-treated cells, more EGFR was present in a tubulovesicular compartment (Figure 2, C and D). In addition to the tubular clusters, in some siRNA-treated cells EGFRs were observed in very thin concentric ring-like structures (Figure 2D, star). In Tsg101-depleted cells multicisternal structures with an

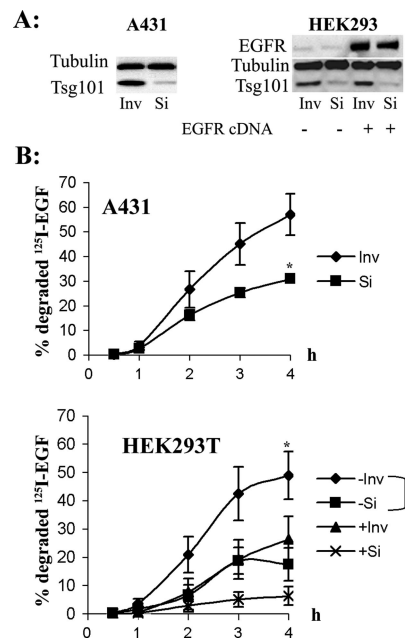


**Figure 1.** Depletion of Tsg101 inhibits EGF degradation. A431 and HEK293T cells were transfected with control (Inv) or siRNA (Si) against Tsg101. Western blots (A) show efficiency of Tsg101 depletion by Oligofectamine in A431 and by nucleofection in HEK293T. HEK293T cells were also transfected with human EGFR cDNA. Tubulin was used as a protein loading control. (B) To assess the kinetics of EGF degradation, cells treated with siRNA (Si), or control oligos (Inv) were incubated with  $^{125}\text{I}$ -EGF for 10 min and chased in ligand-free medium for up to 4 h. The times indicated include the incubation period with EGF. In HEK293T cells, EGFR was either overexpressed (+Inv, +Si) or not (-Inv, -Si). Data represent mean  $\pm$  SEM from at least three independent experiments (\* $p < 0.05$ ).

intercisternal matrix (Figure 2E, arrows) similar to those described by Doyotte *et al.* (2005), also were observed. In contrast to the tubulovesicular compartment, the multicisternal structures contained very few EGFRs (Figure 2E).

To determine how extensive and interconnected the tubulovesicular compartment might be, cells were stimulated with EGF conjugated to HRP. The electron-dense DAB reaction product allows the examination of thick (200-nm) sections, and these showed that control cells contained typical EGF-positive MVBs, but in siRNA-treated cells MVBs were much rarer and more EGF was found in very long tubular structures (Figure 3). These structures had a variable diameter, but most were thin (approximately 50 nm in diameter) and in a single cluster in the pericentriolar region of the cell.

Enlarged vacuoles and tubules could occasionally be seen in the same cell. To investigate the relationship between them, the time course of appearance of EGF in the vacuoles versus the tubules and the effects of efficiency of depletion of Tsg101 were investigated. After incubation with a pulse of fluorescent EGF, followed by ligand-free chase, a clear difference in the distribution of EGF in control and Tsg101-depleted cells could be visualized (Figure 4). In our initial experiments (shown in the previous figures), A431 cells were treated with siRNAs in the presence of Oligofectamine, resulting in >90% depletion of Tsg101. We later found that nucleofection of A431 cells in the presence of siRNAs resulted in more efficient depletion of Tsg101, such that the protein was undetectable even after prolonged exposure of Western blots (Figure 8A). In oligofected (Figure 4A) and

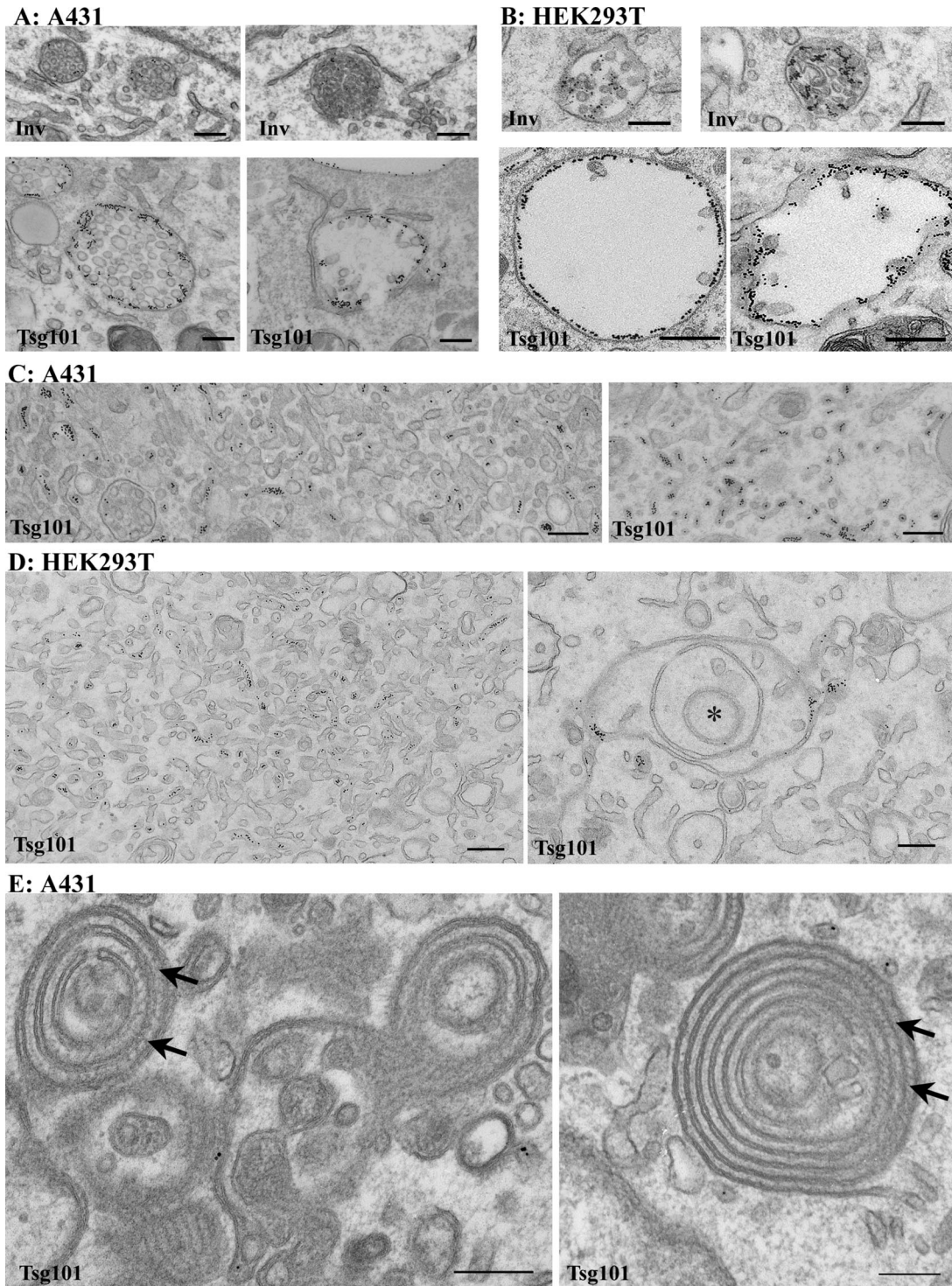


**Figure 2.** Tsg101 depletion modifies the morphology of endosomes. (A–E) Control (Inv) and Tsg101-depleted (Tsg101) A431 and HEK293T cells were incubated with anti-EGFR gold-conjugated antibody and EGF for 2 h at 37°C. Cells were fixed and prepared for transmission electron microscopy (TEM). Micrographs show thin (70-nm) sections. A and B show EGFR-containing MVBs, which tend to be enlarged and contain fewer internal vesicles in Tsg101-depleted cells. C and D show tubulovesicular structures containing EGFR. Star in D shows a ring-like structure containing EGFR. E shows multicisternal structures devoid of EGFR. Arrows indicate the intercisternal matrix. Bars, 200 nm.

nucleofected (Figure 4B) Tsg101-depleted cells, enlarged vacuoles were visible within 30 min of EGF stimulation, but after 1 h of EGF stimulation some cells contained a single large blob of fluorescence. The blobs were more

prominent and present within more cells after 2 h. This change in morphology was specific to the loss of Tsg101, because a second siRNA, which targeted another area of the RNA, gave the same result (see Supplemental Figure

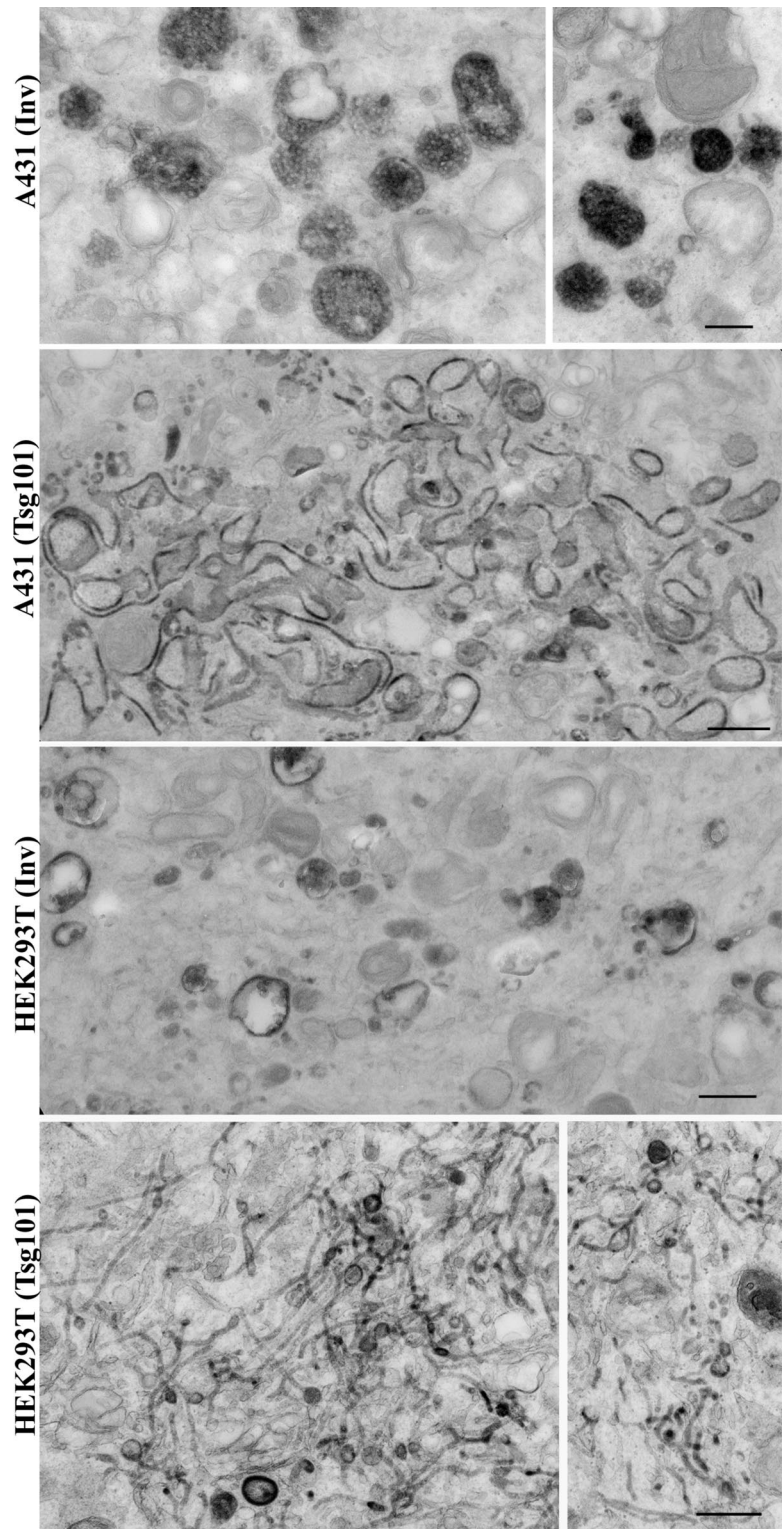


**Figure 3.** EGF is in extensive tubular clusters in Tsg101-depleted cells. Control (Inv) and Tsg101-depleted (Tsg101) A431 and HEK293T cells were stimulated with HRP-EGF at 37°C for 1–2 h. Cells were fixed and incubated with hydrogen peroxide and DAB and were then embedded by standard procedures and prepared for TEM. The electron-dense structures contain DAB reaction product. Micrographs show thick (200-nm) sections. Whereas the majority of EGF is in MVBs in control cells, the majority of EGF is in tubular clusters in Tsg101-depleted cells. Bars, 500 nm.

1). There were fewer enlarged vacuoles, and the blobs were more striking in nucleofected compared with oligofected cells. Thus, appearance of EGF in enlarged vacuoles precedes appearance in the blobs, and the more complete the depletion of Tsg101, the more EGF is in the blobs.

EM showed that the majority of EGFR in EGF stimulated Tsg101-depleted cells was in a tubular cluster and that the

majority of the tubules had a diameter below the resolution of the light microscope. The single blob observed after confocal microscopy of cells loaded with fluorescent EGF was therefore likely to correspond to the tubular cluster observed by EM. To verify that this was the case, siRNA-treated cells were serum-starved and stimulated with Alexa 488-EGF in the presence of anti-EGFR-gold for 2 h. Phase and fluores-

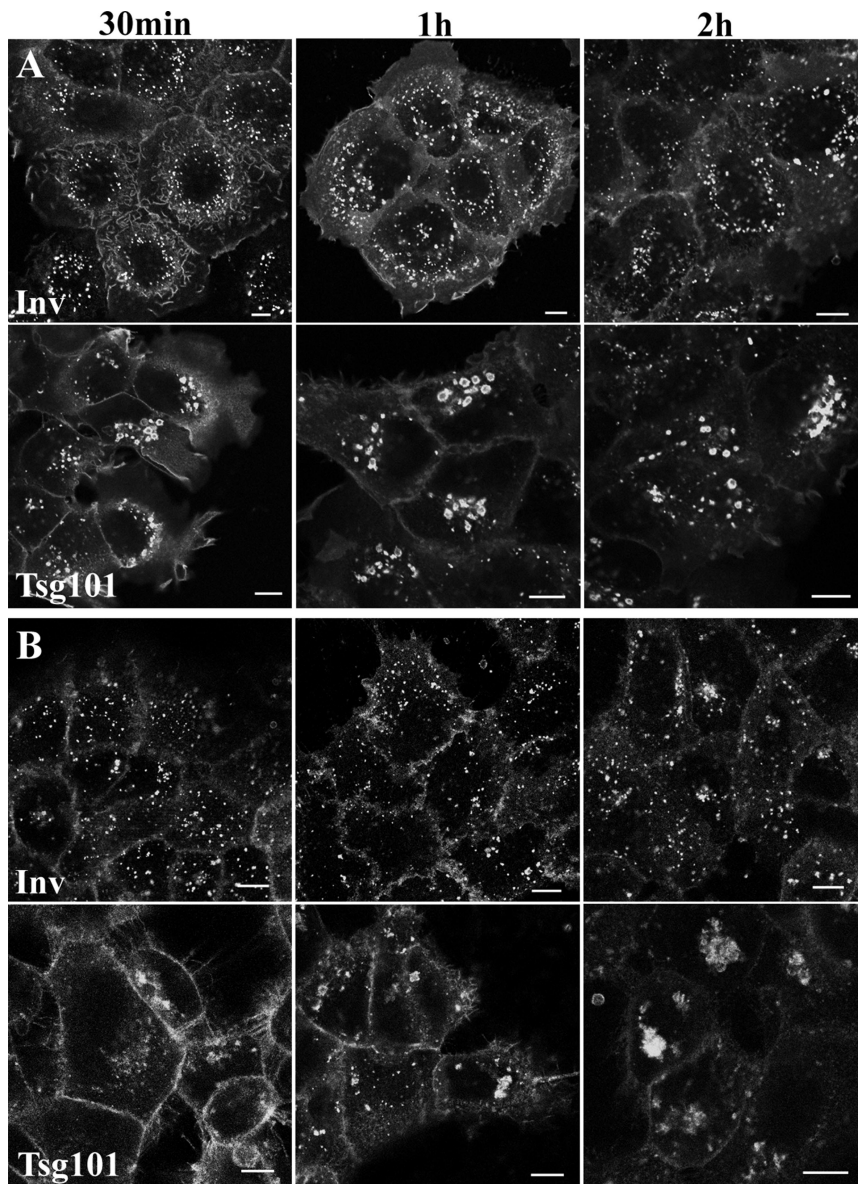


**Figure 4.** Clustering of EGF is enhanced by more effective depletion of Tsg101 and time after EGF stimulation. A431 cells were transfected by control oligo (Inv) or Tsg101 siRNA (Tsg101) using either Oligofectamine (A) or nucleofection (B). Cells were stimulated with Alexa 488-EGF for 15–30 min and chased in serum-free medium. The number of enlarged MVBs is reduced and the clustering more marked in nucleofected versus oligofected cells, and clustering is most marked after 2 h EGF stimulation. Bars, 10  $\mu$ m.

cent images of the cells were taken and then the same cells were processed for EM (Figure 5). As predicted, the fluorescent blob (Figure 5, top, arrows) was indeed a tubular cluster (Figure 5, bottom, arrows). Each 70-nm EM section only contains a small fraction of the depth of the cell shown in the epifluorescence image in Figure 5 (and is also much thinner than the optical confocal sections shown in Figures 4 and 6). However, examination of serial sections through this region demonstrated that the entire area of cytoplasm occupied by the blob contained narrow EGFR-containing ring-tubules in at least some sections. The EGFR containing ring-like structures (Figure 5, stars), along with a multicisternal structure with intercisternal matrix (Figure 5, arrowheads), also were present in the same region, but as before they contained few EGFR and so could not contribute significantly to the signal from fluorescent EGF in the tubular cluster. Enlarged vacuoles containing few internal vesicles were not visible anywhere in these cells that were efficiently depleted of Tsg101.

#### *The Tubules Generated by Tsg101 Depletion Are Modified Early Endosomes*

To determine the identity of the tubular clusters caused by Tsg101 depletion, A431 cells were pulsed with fluorescent EGF, followed by ligand free chase for 2 h and were then fixed, permeabilized, and labeled for the early endosomal marker EEA1 (Figure 6A). In control cells, both EGF and EEA1 were distributed throughout the peripheral cytoplasm. EGF partly colocalized with EEA1 even after a 2-h chase because, due to the high levels of EGFR expression, there is considerable recycling of EGF in A431 cells so that a pulse of EGF is not efficiently chased out of the early endosome. There were also EGF-positive EEA1-negative vacuoles, which were presumably MVBs en route to the lysosome. Tsg101 depletion caused a very striking shift in the distribution of EEA1 to the tubular clusters, where it colocalized with EGF, and there was a marked reduction in the number of EEA1-positive punctae (Figure 6A).

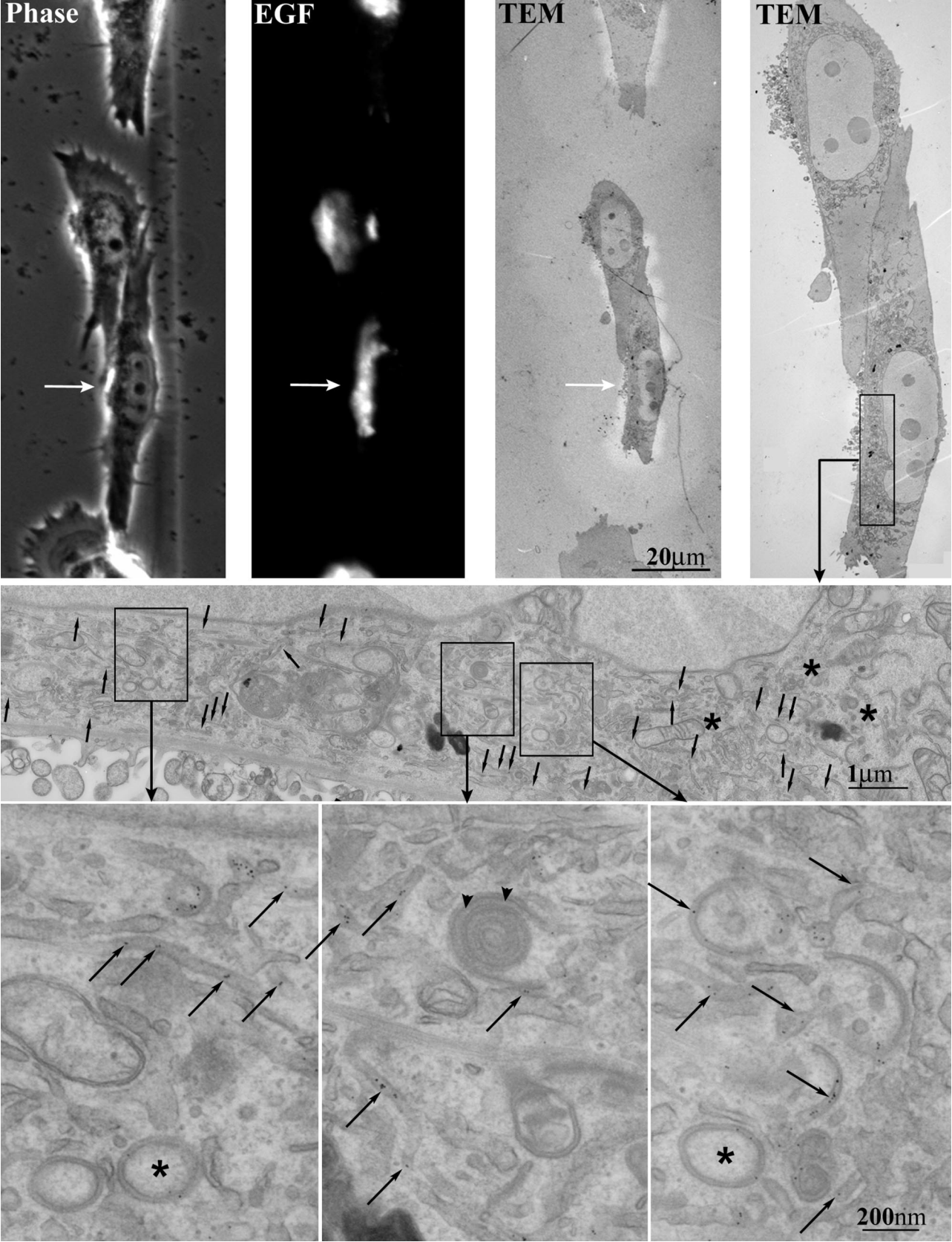


**Figure 5.** EGF-positive blobs observed by light microscopy correspond to the tubular structures observed by EM. A431 cells were nucleofected with Tsg101 siRNA and incubated with Alexa 488-EGF and anti-EGFR gold-conjugated antibody for 2 h. Top, phase, fluorescent, and EM images of transfected cells. The arrows in the top panel show an EGF containing cluster. Bottom, magnified EM images of the same

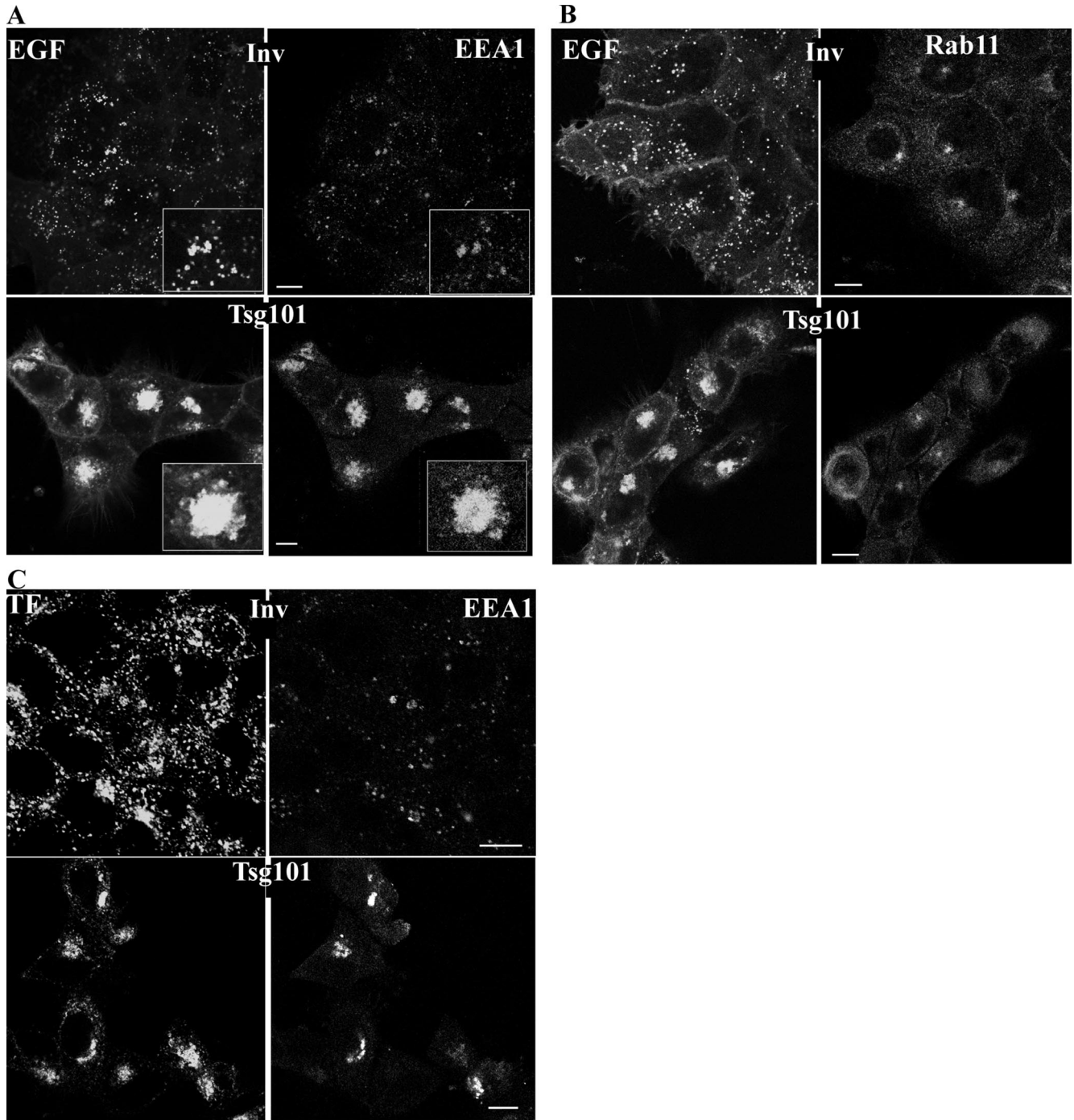


**Figure 6.** Tubular clusters stain for EEA1 and TF but not Rab 11. A431 cells were nucleofected with control oligo (Inv) or Tsg101 siRNA (Tsg101). Cells were stimulated with either fluorescent EGF for 30 min (A and B) and chased for 2 h or stimulated with fluorescent TF for 2 h (C). Cells were fixed and stained for EEA1 (A and C) or Rab11 (B). Tsg101 depletion causes clustering of EEA1 and TF into the same compartment as EGF. EEA1- and TF-positive clusters are reduced but still present in non-EGF-stimulated cells (C). Bars, 10  $\mu$ m.

In control cells, Rab11 stained a single compartment tightly located in the juxtannuclear region, presumably

representing the recycling compartment, as well as showing some peripheral staining (Figure 6B). Tsg101 depletion did not cause any change in the distribution of Rab11, which still stained a juxtannuclear compartment in the same region as the tubular clusters but with a different morphology (Figure 6B). Tsg101 depletion also had no effect on the distribution of Lamp 1 (our unpublished data). We conclude, therefore, that the tubular clusters in

**Figure 5 (cont).** region indicated in the top panel. Arrows point to the EGFR-containing tubular structures (10-nm gold). Stars mark the ring-like structures containing EGFR. The arrowheads in the bottom panels show the intercisternal matrix in a multicisternal structure.

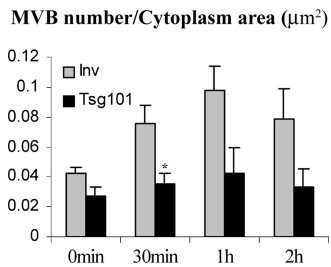


**Figure 7.** Tsg101 depletion reduces MVB formation. A431 cells were nucleofected with control (Inv) or Tsg101 siRNA and incubated with anti-EGFR gold antibody and EGF for 0 min to 2 h. Cells were analyzed by EM (see *Materials and Methods*). There was a small reduction in MVB numbers in the absence of EGF stimulation, and EGF-stimulated MVB formation was abolished. Data shown represent mean  $\pm$  SEM number of MVBs per square micrometer of the cytoplasm from three independent experiments. (\* $p < 0.05$ ).

Tsg101-depleted cells represent a modified early endosome, rather than recycling tubules.

When Tsg101-depleted cells were incubated with fluorescent TF in the absence of EGF, TF also redistributed to the tubular clusters where it costained with EEA1 (Figure 6C). In contrast, in control cells TF was found in many punctae throughout the peripheral cytoplasm, some of which costained with EEA1. This indicates that EGF stimulation is not required for the formation of the tubular clusters. However, the tubular clusters were clearly expanded in the presence of EGF stimulation (compare EEA1 staining in Tsg101-depleted cells in Figure 6, A versus C).

#### Tsg101 Depletion Inhibits Formation of MVBs

As described above, in Tsg101-depleted cells there was a relative increase in association of EGF with tubular clusters, compared with MVBs, with time after EGF stimulation. We therefore quantitated the effects of Tsg101 depletion on MVB number, classifying an MVB as a vacuole with a diameter of  $>200$  nm, containing one or more internal vesicles and lacking lamellar inclusions. We have previously shown that this definition includes both early and late MVBs but excludes the lysosomal compartment in which EGFR are degraded, because that has a multilamellar component (Futter *et al.*, 1996; White *et al.*, 2006). As shown in Figure 7, in control cells the number of MVBs/U cytoplasm increased with EGF stimulation, as found in other cell types (White *et al.*, 2006). However the EGF-stimulated increase in MVB number was abolished by depletion of Tsg101. In serum-starved cells Tsg101 depletion caused a small reduction in the number of MVBs/U cytoplasm, suggesting that Tsg101 is also required for MVB formation in unstimulated cells but that some MVBs may form independently of Tsg101. Thus, both inhibition of MVB formation and tubulation of the early endosome were greatest in EGF-stimulated cells, suggesting that these two changes are related.

#### Hrs Depletion Does Not Mimic Tsg101 Depletion

Because recruitment of Tsg101 to the endosome is thought to be mediated by Hrs, the effects of Hrs depletion on MVB formation were investigated. To compare the effects of Tsg101 and Hrs depletion on EGF traffic, cells were incubated with a 10-min pulse of EGF, surface stripped, and then chased in the presence of unlabeled EGF. The total amount of EGF bound during a 10-min pulse was similar in control, Tsg101-depleted and Hrs-depleted cells, but the percentage of that pulse that

was internalized was reduced approximately threefold in Tsg101-depleted but not Hrs-depleted cells (our unpublished data). Because similar levels of EGF and EGFR seemed to be internalized during longer incubations in control and Tsg101-depleted cells (as shown by the morphological studies), it is likely that Tsg101 depletion has an effect on the initial rate of endocytosis of EGFR but not on the total amount of EGFR internalized. Surprisingly, despite a very efficient (98%) depletion of Hrs (Figure 8A), Hrs depletion caused only a small reduction in EGF degradation such that the percentage of a pulse of internalized EGF degraded after 4 h was reduced 1.5-fold, compared with sixfold after depletion of Tsg101 (Figure 8B). The -fold reduction in EGF degradation caused by Tsg101 depletion was greater in these nucleofected cells than the oligofected cells shown in Figure 1 where the Tsg101 depletion was less complete. The absolute percentages of EGF degraded in control cells differed in Figure 8B, compared with Figure 1, because in the experiments shown in Figure 8B excess unlabeled EGF was included in the chase medium so that recycling could be measured in parallel. Unlabeled EGF displaces recycled ligand from the cell surface so that the fate of only one cycle of EGF is followed. Because of the high expression of EGFR in A431 cells, a large percentage of EGFR is recycled in each round of endocytosis, resulting in a lower percentage of EGFR being degraded in a single round of endocytosis. In the absence of EGF in the chase medium (as in the experiments shown in Figure 1), multiple rounds of endocytosis and recycling are followed resulting in a higher percentage of the initial pulse of EGF being degraded.

As shown in Figure 8B, inhibition of EGF degradation was accompanied by enhanced recycling of EGF in both Tsg101-depleted and Hrs-depleted cells. Tsg101-depleted but not Hrs-depleted cells showed a small increase in the amount of EGF retained within the cells. In parallel experiments TF recycling was also slightly enhanced in Tsg101-depleted cells (Supplemental Figure 2).

In Hrs-depleted cells, EGF was found in enlarged vacuoles (Figure 8C, arrow). Vacuolar enlargement was due to the loss of Hrs, because a second siRNA that targeted another area of the RNA gave the same result (Supplemental Figure 1). Some of these enlarged vacuoles stained weakly for TF and EEA1 (Figure 8D), but there was no evidence of redistribution of TF or EEA1 to tubular clusters. The enlarged EGF-positive vacuoles showed a wider distribution than the tight cluster of tubules in Tsg101-depleted cells (Figure 8, C and D), and EGF was not found in tubular clusters by either light microscopy or EM (see below).

Although the depletion of Hrs was very efficient, a small amount of Hrs was still detectable, raising the possibility that a small amount of endosomal-associated Hrs might remain in Hrs-depleted cells and that this might be sufficient to prevent the formation of tubular clusters. Immunofluorescent staining with anti-Hrs antibody showed that although some endosomal staining was present in some cells, cells that had very enlarged EGF-containing vacuoles and no detectable Hrs were also observed, indicating that the vacuolar enlargement did not arise from only a partial depletion of Hrs (Figure 8C).

EM analysis showed that in Hrs-depleted cells, EGFRs were found in enlarged MVBs with few internal vesicles, although smaller MVBs with more internal vesicles could also be found in the same cells (Figure 9 and Supplemental Figure 3). Tubular clusters, ring-like structures, and multicisternal structures were never observed in Hrs-depleted cells. To quantitate the effects of Hrs depletion on MVB size and inward vesiculation, random MVBs were counted, whether or not they contained EGFRs. In the absence of EGF

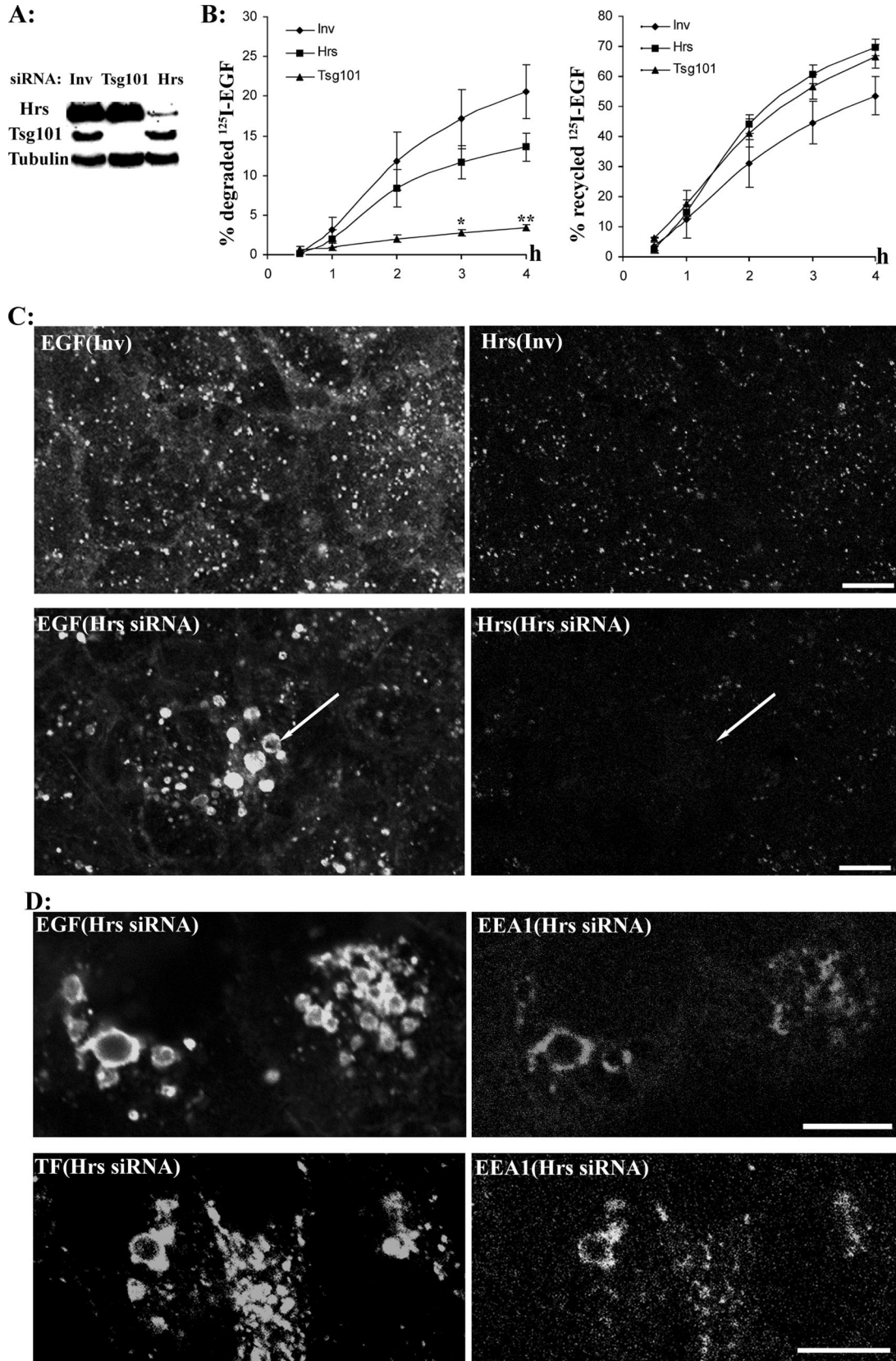


**Figure 8.** Hrs depletion causes the enlargement of endosomes and a moderate reduction in EGF degradation. (A and B) A431 cells were nucleofected with control (Inv) oligo or siRNA against Tsg101 or Hrs. (A) Western blot shows efficiency of Tsg101 and Hrs depletion by nucleofection. Tubulin was used as a loading control. (B) Kinetics of EGF degradation and recycling. Hrs- and Tsg101-depleted cells were incubated with <sup>125</sup>I-EGF for 10 min and chased with unlabeled EGF. EGF degradation was modestly reduced in Hrs-depleted cells but was

stimulation, MVBs were enlarged in both Hrs- and Tsg101-depleted cells, although the degree of enlargement was greater in Hrs-depleted cells (Figure 10). After 2 h of EGF stimulation the area of MVBs in Hrs-depleted cells was 4.6-fold increased compared with control cells and the majority of MVBs contained EGFR (73%). In contrast MVBs in Tsg101-depleted cells were no longer enlarged after 2-h EGF stimulation and only 57% of them contained EGFRs.

Possible reasons for vacuolar enlargement include inhibition of inward vesiculation, inhibition of exit from the vacuoles, or fusion of vacuoles with each other. Although there was an inhibition of inward vesiculation in Hrs-depleted cells (see below) it was insufficient to explain the vacuolar enlargement. Recycling of EGF was not inhibited in Hrs-depleted cells, suggesting that exit of at least endocytosed ligands was not prevented. Homotypic fusion between MVBs would decrease the number of MVBs/U cytoplasm but not the area of cytoplasm occupied by MVBs. As shown in Figure 10, in EGF-stimulated Tsg101-depleted cells both the number of MVBs/U cytoplasm and the area of cytoplasm occupied by MVBs were reduced, whereas in Hrs-depleted cells only the number of MVBs was reduced. The area of cytoplasm occupied by MVBs was actually increased, probably reflecting both an increase in fusion events and an inhibition of inward vesiculation. We were unable to quantify fusion events between MVBs and it is not clear at which stage fusion was occurring. However, profiles suggestive of fusion between normal-sized MVBs and enlarged MVBs were observed in Hrs-depleted cells (Figure 9).

When vacuoles are greatly enlarged quantitation of the numbers of internal vesicles in thin sections becomes complicated, because the number of sections that contain an enlarged MVB increases. We therefore quantified the number of internal vesicles/MVB area, rather than the number of internal vesicles/MVB, in Hrs- and Tsg101-depleted cells. In Hrs-depleted cells, the density of internal vesicles within MVBs was reduced whether or not the cells were stimulated with EGF, and after 2 h of EGF stimulation the density of internal vesicles within MVBs was reduced 5.2-fold, compared with control cells (Figure 10). Correcting for the slightly increased cytoplasmic area occupied by MVBs, this indicates a 3.4-fold decrease in the numbers of internal vesicles made in Hrs-depleted cells. Although the internal vesicle density in Tsg101-depleted cells was not reduced as much as in Hrs-depleted cells, correcting for the considerably reduced cytoplasmic area occupied by MVBs in Tsg101-depleted cells, internal vesicle formation was reduced 3.6-fold after 2 h of EGF stimulation.

Together with the demonstration that a considerable proportion of endocytosed EGF can be delivered to the lysosome in Hrs-depleted cells, these data indicate that Hrs depletion allows the formation of MVBs that retain the ability to fuse with the lysosome, but the MVBs formed are

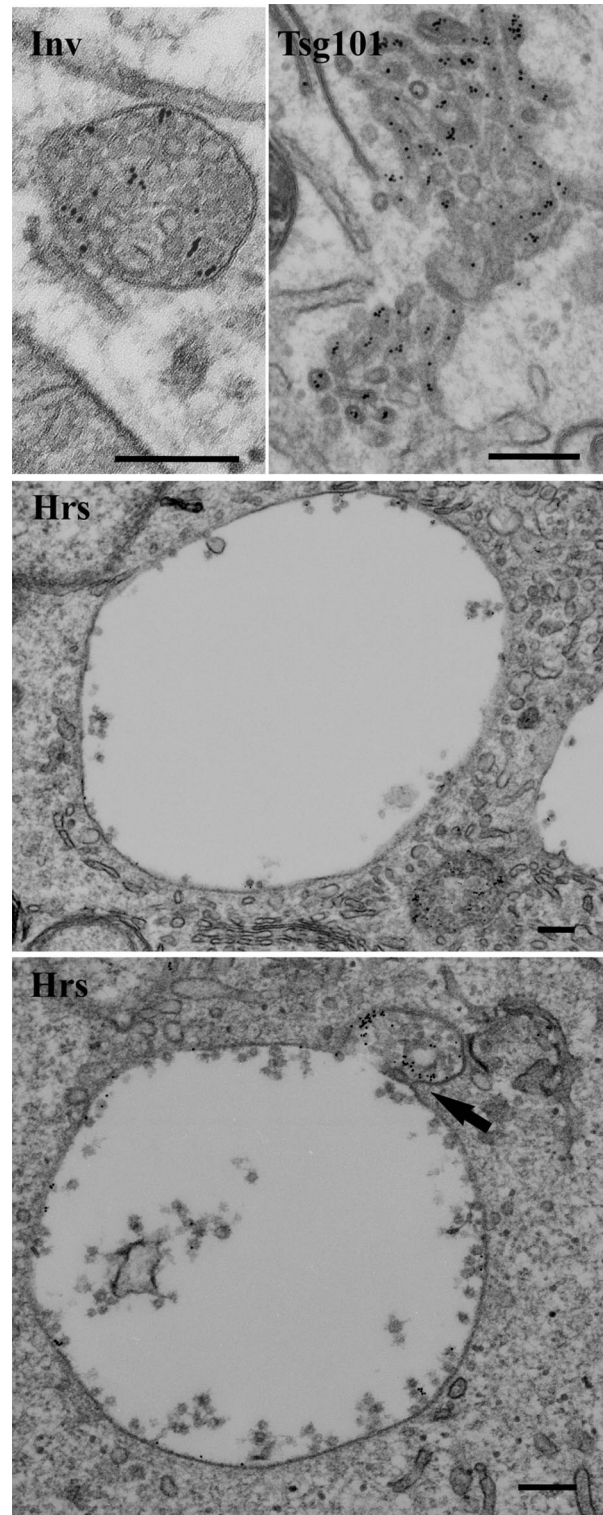


**Figure 9.** Hrs depletion causes the enlargement of endosomes. Control (Inv), Hrs-, and Tsg101-depleted A431 cells were incubated with anti-EGFR gold-conjugated antibody and EGF for 2 h. Micrographs show thin (70-nm) sections. Note that MVBs in Hrs-depleted cells are greatly enlarged and have fewer internal vesicles. Arrow shows a profile suggestive of a small MVB fusing with a larger one. Bars, 200 nm.

**Figure 8 (cont).** almost abolished after Tsg101 depletion. Recycling of EGF was enhanced in Hrs- and Tsg101-depleted cells. Data represent mean  $\pm$  SEM from three independent experiments (\*\* $p < 0.001$ , \* $p < 0.05$ ). (C) Confocal images of control and Hrs-depleted A431 cells. Cells were serum starved and stimulated with Alexa 488-EGF for 2 h. Cells were fixed and stained for endogenous Hrs. The arrow shows an area containing enlarged endosomes devoid of Hrs. Bars, 10  $\mu$ m. (D) Confocal images of Hrs-depleted A431 cells. Cells were serum starved and stimulated with either Alexa 555-TF for 2 h or Alexa 488-EGF for 30 min and chased for 2 h. Cells were fixed and stained for EEA1. There is some staining of enlarged endosomes with EEA1 and TF, but no tubular clusters were observed. Bars, 10  $\mu$ m.

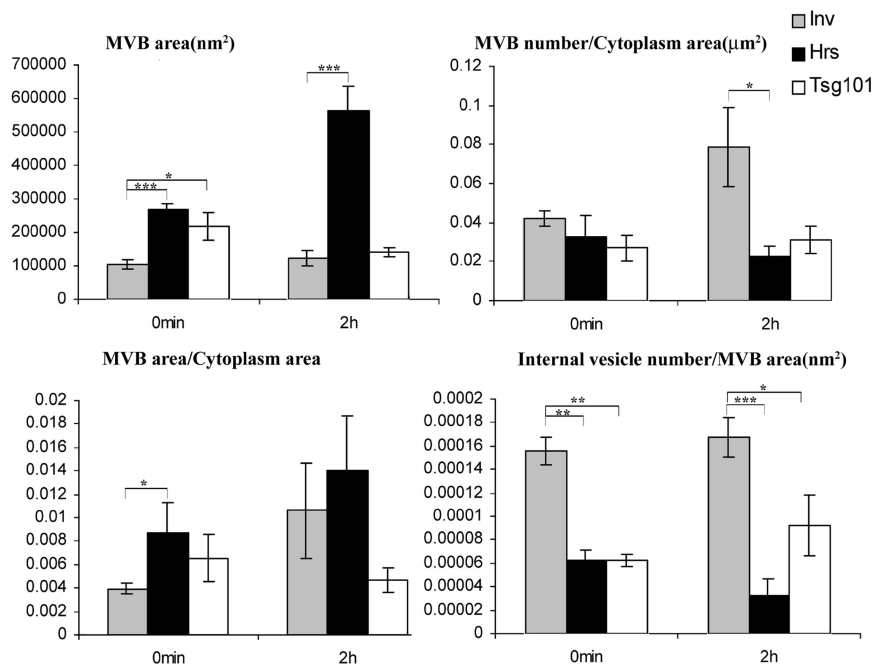


**Figure 10.** Quantification of EM analysis of Tsg101- and Hrs-depleted cells. Control (Inv) (shaded columns), Hrs (filled columns), or Tsg101 (open columns) siRNA-treated A431 cells were incubated with anti-EGFR gold antibody and EGF for 0 and 2 h. Cells were analyzed by EM (see *Materials and Methods*). For comparison, the number of MVBs/ $\mu\text{m}^2$  of cytoplasm shown in Figure 7 for control and Tsg101-depleted cells is also included. Data represent mean  $\pm$  SEM from at least three independent experiments (\* $p < 0.05$ , \*\* $p < 0.001$ , \*\*\* $p < 0.0001$ ).

larger and fewer in number, probably because of homotypic fusion and inhibition of inward vesiculation.

## DISCUSSION

### *Tsg101 Depletion Causes the Early Endosome of Mammalian Cells to Form a Tubular Cluster*

As observed previously (Babst *et al.*, 2000), Tsg101 depletion caused a reduction in the efficiency of EGF degradation, consistent with a role in the selection of cargo for retention in MVBs. Yeast and mammalian studies suggest that components of ESCRT-I also play a role in regulating the structure of endocytic compartments. In some Tsg101-depleted A431 and HEK293T cells, we observed multicisternal structures with an intercisternal matrix as described by Doyotte *et al.* (2005). Doyotte *et al.* (2005) showed that these structures were endosomal, because they could be loaded with TF conjugated to HRP. However, we found that in EGF-stimulated cells, these structures contained very few EGF receptors. At early time points after EGF stimulation, EGFRs were found in enlarged vacuoles but after prolonged stimulation, the majority of EGFRs were found in a striking cluster of tubules in Tsg101-depleted cells. Occasionally these tubules were arranged in concentric ring-like structures, but most were in a cluster with a disorganized appearance. These structures were most readily observed in thick sections of cells loaded with EGF conjugated to HRP, not reported by Doyotte *et al.* (2005). Their pericentriolar location, small diameter, and accessibility to endocytosed TF resembled recycling tubules (Yamashiro *et al.*, 1984; Hopkins *et al.*, 1994). However, the tubular clusters stained strongly for EEA1 and poorly for Rab11. EEA1 localizes to Rab5-positive vacuolar early endosomes and shows little overlap with Rab11-positive tubular recycling endosomes (Trischler *et al.*, 1999; Sonnichsen *et al.*, 2000). We conclude therefore that the tubular clusters are modified domains of the early sorting endosome. Doyotte *et al.* (2005) also found a redistribution of EEA1-positive early endosomes in Tsg101-depleted cells, accompanied by major morphological changes within the

early endosome. They concluded that there was a generalized defect in the vacuolar and tubular domain structure of the early endosome, accompanied by defective sorting to both degradative and recycling pathways. We found that despite the changes in the morphology of the early endosome after Tsg101 depletion, that are most dramatic in EGF-stimulated cells, the domain structure of the endosome is not entirely lost, because EEA1 and Rab11 maintain separate distributions. Furthermore, we found that recycling from the tubular early endosome still occurred in Tsg101-depleted cells. Enhanced EGF and TF recycling under conditions of Tsg101 depletion suggests that the tubulation of the early endosome is not due to a failure of recycling vesicles to detach from the early endosome.

### *Tsg101 Is Required for the Formation of MVBs*

Tsg101-depleted cells had a smaller number of MVBs both with and without EGF stimulation. The difference in MVB number in control versus Tsg101-depleted cells was much greater in EGF-stimulated cells, such that EGF-stimulated MVB formation was abolished. How could Tsg101 be regulating the numbers of MVBs? In this study, all MVBs that have at least one internal vesicle in cross-section have been counted, and this allows us to distinguish between MVB formation (numbers of MVBs/U cytoplasm) and internal vesicle formation (numbers of internal vesicles/MVB). If we defined an MVB as a vacuole with many internal vesicles, then a reduction in the numbers of MVBs could well reflect a reduction in inward vesiculation (because a reduced number of vacuoles would have the threshold number of internal vesicles). With our definition of an MVB, although a minimal amount of internal vesicle formation has to occur for a vacuole to be defined as an MVB, it is possible to have a major effect on inward vesiculation without affecting MVB number, as shown in our previous studies where loss of annexin 1 abolished EGF-stimulated inward vesiculation without affecting EGF-stimulated MVB formation (White *et al.*, 2006). The reduced number of MVBs in Tsg101-depleted cells is unlikely, therefore, to be solely due to an inhibition of inward

vesiculation, leading to fewer vacuoles being scored as MVBs. Furthermore, a failure to inwardly vesiculate would not directly cause the tubulation of the early endosome that we observed. Tubulation is not an inevitable consequence of excessive vacuolar enlargement, because tubulation of the early endosome was not observed after vacuolar enlargement in wortmannin-treated cells (Futter *et al.*, 2001) or in cells depleted of Hrs (see below).

Given that MVB biogenesis is initiated when the perimeter membrane of vacuolar domains within the early endosome inwardly invaginates to form internal vesicles, a reduction in the number of MVBs is likely to reflect a reduction in the formation or stability of vacuolar domains within the early endosome. The demonstration that EEA1 localizes to the tubules induced by Tsg101 depletion indicates a loss of vacuolar domains within the early endosome. EGF-containing vacuolar domains, although reduced in number, were initially present and even enlarged at early time points after EGF stimulation, but the enlarged vacuoles were consumed by the tubulation of the early endosome so that at later time points after EGF stimulation, the vacuolar enlargement was lost. Although tubular clusters were present in the absence of EGF stimulation, they were considerably expanded in EGF-stimulated Tsg101-depleted cells. Together, these data strongly suggest that Tsg101 regulates the formation and stability of the vacuolar domains of early endosomes from which MVBs form and that EGF stimulation of MVB biogenesis increases vacuolar instability in the absence of Tsg101.

Thus, two processes in MVB biogenesis can be resolved: 1) stable vacuole formation and 2) internal vesicle formation. Tsg101-mediated stable vacuole formation is likely to be a requirement for the efficient generation of internal vesicles within MVB, and so whether Tsg101 plays a further role in inward vesiculation is not possible to determine from these data.

#### ***Tsg101-mediated MVB Formation Is Independent of Hrs***

That depletion of Hrs had only a modest effect on EGF degradation, compared with the almost complete inhibition of EGF degradation obtained by depletion of Tsg101, was the first indication that MVBs can still form in Hrs-depleted cells, because MVB-lysosome fusion is the only mechanism thus far described for the delivery of EGF to the lysosome.

Although the morphological phenotypes of Hrs and Tsg101 depletion were superficially similar in unstimulated cells, EGF stimulation revealed major differences in their phenotypes. After Hrs depletion, EGF/EGFR was found in enlarged vacuoles containing few internal vesicles, and in no cells were tubular clusters observed. Unlike in Tsg101-depleted cells, there was no major effect of Hrs depletion on the distribution of TF or EEA1. There was a decrease in the number of MVBs/U cytoplasm in both Tsg101- and Hrs-depleted cells, but the MVBs formed differed: 1) MVBs in Hrs-depleted cells were much larger so that the total area of cytoplasm occupied by MVBs was greater than that in control cells, whereas there was very little MVB size increase after Tsg101 depletion, such that the area of cytoplasm occupied by MVBs was greatly decreased compared with control cells; 2) in Hrs but not Tsg101-depleted cells profiles suggestive of fusion between normal-sized and -enlarged MVBs were observed; and 3) a greater proportion of MVBs formed in Hrs-depleted cells contained EGFR, compared with Tsg101-depleted cells.

The differences between the effects of depletion of Tsg101 and that of Hrs cannot be explained by differences in the efficiency of depletion of the two molecules. There was a

detectable amount of Hrs remaining after siRNA-mediated depletion, albeit at ~2% of the level found in control cells, and in some cells endosome-associated Hrs could still be detected. However, in cells with no detectable Hrs EGF-positive vacuoles tended to be particularly large, and there were no tubular clusters. These data are consistent with the demonstration of enlarged endosomes in tissues of Hrs knockout mouse embryos and fibroblasts derived from them (Komada and Soriano, 1999; Kanazawa *et al.*, 2003).

How can these data be reconciled with a number of studies showing roles for Hrs in 1) the concentration of ubiquitinated proteins destined for lysosomal delivery (Raiborg *et al.*, 2002; Sachse *et al.*, 2002; Bilodeau *et al.*, 2003; Urbe *et al.*, 2003), 2) the recruitment of Tsg101 to endosomal membranes (Bache *et al.*, 2003), and 3) MVB formation (Bache *et al.*, 2003)? First, we do observe a modest inhibition of EGF degradation in Hrs-depleted cells similar to that shown by Lu *et al.*, (2003) for EGFR and by Hammond *et al.* (2003) for Met. Similarly, the impairment of EGFR degradation observed in fibroblasts derived from Hrs knockout mouse embryos was only partial (Kanazawa *et al.*, 2003). Although in keeping with a role for Hrs in concentrating ubiquitinated proteins destined for lysosomal delivery, these data suggest other ubiquitin binding proteins, such as GGA3 (Puertollano and Bonifacino, 2004), might perform this role in the absence of Hrs. Second, direct interaction between Hrs and Tsg101 has been clearly demonstrated in several studies (Bache *et al.*, 2003; Katzmann *et al.*, 2003; Lu *et al.*, 2003) and that interaction shown to be important for mediating membrane association of Tsg101. However, depletion of Hrs only inhibits membrane association of Tsg101 by 50% (Bache *et al.*, 2003), suggesting that additional mechanisms exist to promote membrane association of Tsg101. Our studies indicate that the pool of Tsg101 that mediates stable vacuole formation does so independently of Hrs. Third, where depletion of Hrs was reported to inhibit MVB formation (Bache *et al.*, 2003) MVBs were classified as vacuoles with many internal vesicles and so, in keeping with our results, the effect of Hrs depletion may have been primarily on internal vesicle formation, rather than MVB formation.

Our study suggests that the interaction between Tsg101 and Hrs could be important for coupling stable vacuole formation to the accumulation of internal vesicles within MVB and is consistent with previous studies indicating a role for Hrs in inward vesiculation in *Drosophila* Garland cells (Lloyd *et al.*, 2002) and in mammalian cells (Urbe *et al.*, 2003). That in some systems overexpression of Hrs can mimic the effects of Hrs depletion (Bishop *et al.*, 2002; Urbe *et al.*, 2003) suggests that the amount of Hrs relative to Tsg101 is important in the regulation of inward vesiculation.

#### ***The Role of Hrs in Promoting Membrane Invagination within MVBs***

We have previously found that annexin 1 is required for EGF-stimulated inward vesiculation (White *et al.*, 2006) but not for inward vesiculation in unstimulated cells. In contrast, Hrs depletion inhibits internal vesicle formation in unstimulated cells and also prevents EGF-stimulated inward vesiculation. The phenotype we observe with Hrs depletion bears a striking resemblance to that we have observed after inhibition of Vps34 (Futter *et al.*, 2001), which caused the generation of greatly enlarged MVBs with fewer internal vesicles and only a small inhibition of EGF degradation, suggesting that the effects of inhibition of Vps34-mediated generation of phosphatidylinositol 3-phosphate on inward vesiculation may be mediated through inhibition of recruitment of Hrs. As was the case

with vacuolar enlargement induced by inhibition of Vps34, the vacuolar enlargement induced by depletion of Hrs cannot be explained solely through an inhibition of inward vesiculation. Because the area of cytoplasm occupied by MVBs in Hrs-depleted cells was not decreased compared with control cells, our data would be consistent with a role for Hrs in the inhibition of homotypic fusion between endosomes. Although we have been unable to quantitate the extent of such fusion in Hrs-depleted cells, the previous demonstration that Hrs prevents homotypic endosome fusion *in vitro* by binding to SNAP-25 (synaptosome-associated protein of 25 kDa) and preventing the formation of an endosomal SNARE (soluble N-ethylmaleimide-sensitive factor attachment protein receptor) complex would be consistent with this hypothesis (Sun *et al.*, 2003).

An inhibition of exit of membrane from the vacuole could also contribute to vacuolar enlargement. Two recent studies have identified a role for Hrs in recycling of endocytosed proteins. Cargo specific inhibition of recycling of the G protein-coupled receptor, the  $\beta$ 2-adrenergic receptor, was observed in cells depleted of Hrs and in this case the receptor accumulated in EEA1-positive vacuoles (Hanyaloglu *et al.*, 2005). Rapid recycling of transferrin was shown to require an Hrs-containing complex that also included  $\alpha$  actinin, BERP, and myosin V (Yan *et al.*, 2005). Disruption of this complex caused a re-routing of transferrin via a slower recycling route that involved recycling tubules. Although the recycling cargo are not the same and the stage at which Hrs acts may not be the same, both these studies suggest that Hrs has roles in membrane protein recycling that involve interactions with proteins that are distinct from the ESCRT family. Furthermore, although we found that EGF recycling was enhanced in Hrs-depleted cells, we cannot rule out the possibility that exit of some membrane components from vacuoles may contribute to the vacuolar enlargement in Hrs-depleted cells.

By using EGF stimulation to promote MVB formation and inward vesiculation within MVB, we have been able to resolve distinct steps where Tsg101 and Hrs operate. Tsg101 promotes the formation of stable vacuolar domains within the early endosome that become MVBs. Hrs promotes the accumulation of internal vesicles within those vacuoles. Recently, the melanosomal protein pmel17 was shown to be targeted to the internal vesicles of MVBs independently of both Tsg101 and Hrs (Theos *et al.*, 2006). Furthermore, certain G protein-coupled receptors are delivered to the lysosome independently of Tsg101 (Hislop *et al.*, 2004) or independently of both Tsg101 and Hrs (Gullapalli *et al.*, 2006). Thus, it would seem that in mammalian cells there are multiple routes to the lysosome and more than one mechanism underlying the formation of MVBs and the internal vesicles within them. A major future challenge is to determine the relationship between MVB formation and inward vesiculation that depend on Tsg101 and Hrs, respectively, and ESCRT-independent mechanisms and how they are coordinated to fulfill the specialized requirements of mammalian cells, such as the ability to respond to growth factor stimulation and to make melanosomes.

## ACKNOWLEDGMENTS

We thank the Association for International Cancer Research, Cancer Research UK, the Wellcome Trust, the Medical Research Council, and Fight for Sight for supporting this work.

## REFERENCES

- Babst, M. (2005). A protein's final ESCRT. *Traffic* 6, 2–9.
- Babst, M., Katzmann, D. J., Estepa-Sabal, E. J., Meerloo, T., and Emr, S. D. (2002a). Escrt-III: an endosome-associated heterooligomeric protein complex required for mvb sorting. *Dev. Cell* 3, 271–282.
- Babst, M., Katzmann, D. J., Snyder, W. B., Wendland, B., and Emr, S. D. (2002b). Endosome-associated complex, ESCRT-II, recruits transport machinery for protein sorting at the multivesicular body. *Dev. Cell* 3, 283–289.
- Babst, M., Odorizzi, G., Estepa, E. J., and Emr, S. D. (2000). Mammalian tumor susceptibility gene 101 (TSG101) and the yeast homologue, Vps23p, both function in late endosomal trafficking. *Traffic* 1, 248–258.
- Bache, K. G., Brech, A., Mehlum, A., and Stenmark, H. (2003). Hrs regulates multivesicular body formation via ESCRT recruitment to endosomes. *J. Cell Biol.* 162, 435–442.
- Bilodeau, P. S., Winistorfer, S. C., Kearney, W. R., Robertson, A. D., and Piper, R. C. (2003). Vps27-Hse1 and ESCRT-I complexes cooperate to increase efficiency of sorting ubiquitinated proteins at the endosome. *J. Cell Biol.* 163, 237–243.
- Bishop, N., Horman, A., and Woodman, P. (2002). Mammalian class E vps proteins recognize ubiquitin and act in the removal of endosomal protein-ubiquitin conjugates. *J. Cell Biol.* 157, 91–101.
- DeMey, J. (1986). The preparation and use of gold probes. In: *Practical Applications in Pathology and Biology*, ed. J. M. Polak and S. Van Noorden, Bristol, United Kingdom: Wright.
- Doyotte, A., Russell, M.R.G., Hopkins, C. R., and Woodman, P. G. (2005). Depletion of TSG101 forms a mammalian 'class E' compartment: a multicisternal early endosome with multiple sorting defects. *J. Cell Sci.* 118, 3003–3017.
- Futter, C. E., Collinson, L. M., Backer, J. M., and Hopkins, C. R. (2001). Human VPS34 is required for internal vesicle formation within multivesicular endosomes. *J. Cell Biol.* 155, 1251–1264.
- Futter, C. E., Pearse, A., Hewlett, L. J., and Hopkins, C. R. (1996). Multivesicular endosomes containing internalized EGF-EGF receptor complexes mature and then fuse directly with lysosomes. *J. Cell Biol.* 132, 1011–1023.
- Garrus, J. E., *et al.* (2001). Tsg101 and the vacuolar protein sorting pathway are essential for HIV-1 budding. *Cell* 107, 55–65.
- Graham, R. C., Jr., and Karnovsky, M. J. (1966). Glomerular permeability. Ultrastructural cytochemical studies using peroxidases as protein tracers. *J. Exp. Med.* 124, 1123–1134.
- Gruenberg, J., and Stenmark, H. (2004). The biogenesis of multivesicular endosomes. *Nat. Rev. Mol. Cell Biol.* 5, 317–323.
- Gullapalli, A., Wolfe, B. L., Griffin, C. T., Magnuson, T., and Trejo, J. (2006). An essential role for SNX1 in lysosomal sorting of protease-activated receptor-1, evidence for retromer-, Hrs-, and Tsg101-independent functions of sorting nexins. *Mol. Biol. Cell* 17, 1228–1238.
- Hammond, D. E., Carter, S., McCullough, J., Urbe, S., Vande Woude, G., and Clague, M. J. (2003). Endosomal dynamics of Met determine signaling output. *Mol. Biol. Cell* 14, 1346–1354.
- Hanyaloglu, A. C., McCullagh, E., and von Zastrow, M. (2005). Essential role of Hrs in a recycling mechanism mediating functional resensitization of cell signaling. *EMBO J.* 24, 2265–2283.
- Hislop, J. N., Marley, A., and Von Zastrow, M. (2004). Role of mammalian vacuolar protein-sorting proteins in endocytic trafficking of a non-ubiquitinated G protein-coupled receptor to lysosomes. *J. Biol. Chem.* 279, 22522–22531.
- Hopkins, C. R., Gibson, A., Shipman, M., Strickland, D. K., and Trowbridge, I. S. (1994). In migrating fibroblasts, recycling receptors are concentrated in narrow tubules in the pericentriolar area, and then routed to the plasma membrane of the leading lamella. *J. Cell Biol.* 125, 1265–1274.
- Kanazawa, C., Morita, E., Yamada, M., Ishii, N., Miura, S., Asao, H., Yoshimori, T., and Sugamura, K. (2003). Effects of deficiencies of STAMs and Hrs, mammalian class E Vps proteins, on receptor downregulation. *Biochem. Biophys. Res. Commun.* 309, 848–856.
- Katzmann, D. J., Babst, M., and Emr, S. D. (2001). Ubiquitin-dependent sorting into the multivesicular body pathway requires the function of a conserved endosomal protein sorting complex, ESCRT-I. *Cell* 106, 145–155.
- Katzmann, D. J., Odorizzi, G., and Emr, S. D. (2002). Receptor downregulation and multivesicular-body sorting. *Nat. Rev. Mol. Cell Biol.* 3, 893–905.
- Katzmann, D. J., Stefan, C. J., Babst, M., and Emr, S. D. (2003). Vps27 recruits ESCRT machinery to endosomes during MVB sorting. *J. Cell Biol.* 162, 413–423.
- Komada, M., and Soriano, P. (1999). Hrs, a FYVE finger protein localized to early endosomes, is implicated in vesicular traffic and required for ventral folding morphogenesis. *Genes Dev.* 13, 1475–1485.

- Lloyd, T. E., Atkinson, R., Wu, M. N., Zhou, Y., Pennetta, G., and Bellen, H. J. (2002). Hrs regulates endosome membrane invagination and tyrosine kinase receptor signaling in *Drosophila*. *Cell* 108, 261–269.
- Lu, Q., Hope, L. W., Brasch, M., Reinhard, C., and Cohen, S. N. (2003). TSG101 interaction with HRS mediates endosomal trafficking and receptor down-regulation. *Proc. Natl. Acad. Sci. USA* 100, 7626–7631.
- Martin-Serrano, J., Zang, T., and Bieniasz, P. D. (2001). HIV-1 and Ebola virus encode small peptide motifs that recruit Tsg101 to sites of particle assembly to facilitate egress. *Nat. Med.* 7, 1313–1319.
- Mullock, B. M., Bright, N. A., Fearon, C. W., Gray, S. R., and Luzio, J. P. (1998). Fusion of lysosomes with late endosomes produces a hybrid organelle of intermediate density and is NSF dependent. *J. Cell Biol.* 140, 591–601.
- Puertollano, R., and Bonifacio, J. S. (2004). Interactions of GGA3 with the ubiquitin sorting machinery. *Nat. Cell Biol.* 6, 244–251.
- Raiborg, C., Bache, K. G., Gillooly, D. J., Madshus, I. H., Stang, E., and Stenmark, H. (2002). Hrs sorts ubiquitinated proteins into clathrin-coated microdomains of early endosomes. *Nat. Cell Biol.* 4, 394–398.
- Raymond, C. K., Howald-Stevenson, I., Vater, C. A., and Stevens, T. H. (1992). Morphological classification of the yeast vacuolar protein sorting mutants: evidence for a prevacuolar compartment in class E vps mutants. *Mol. Biol. Cell* 3, 1389–1402.
- Rieder, S. E., Banta, L. M., Kohrer, K., McCaffery, J. M., and Emr, S. D. (1996). Multilamellar endosome-like compartment accumulates in the yeast vps28 vacuolar protein sorting mutant. *Mol. Biol. Cell* 7, 985–999.
- Sachse, M., Strous, G. J., and Klumperman, J. (2004). ATPase-deficient hVPS4 impairs formation of internal endosomal vesicles and stabilizes bilayered clathrin coats on endosomal vacuoles. *J. Cell Sci.* 117, 1699–1708.
- Sachse, M., Urbe, S., Oorschot, V., Strous, G. J., and Klumperman, J. (2002). Bilayered clathrin coats on endosomal vacuoles are involved in protein sorting toward lysosomes. *Mol. Biol. Cell* 13, 1313–1328.
- Sonnichsen, B., De Renzis, S., Nielsen, E., Rietdorf, J., and Zerial, M. (2000). Distinct membrane domains on endosomes in the recycling pathway visualized by multicolor imaging of Rab4, Rab5, and Rab11. *J. Cell Biol.* 149, 901–914.
- Sun, W., Yan, Q., Vida, T. A., and Bean, A. J. (2003). Hrs regulates early endosome fusion by inhibiting formation of an endosomal SNARE complex. *J. Cell Biol.* 162, 125–137.
- Theos, A. C., Truschel, S. T., Tenza, D., Hurbain, I., Harper, D. C., Berson, J. F., Thomas, P. C., Raposo, G., and Marks, M. S. (2006). A luminal domain-dependent pathway for sorting to intraluminal vesicles of multivesicular endosomes involved in organelle morphogenesis. *Dev. Cell* 10, 343–354.
- Trischler, M., Stoorvogel, W., and Ullrich, O. (1999). Biochemical analysis of distinct Rab5- and Rab11-positive endosomes along the transferrin pathway. *J. Cell Sci.* 112, 4773–4783.
- Urbe, S., Sachse, M., Row, P. E., Preisinger, C., Barr, F. A., Strous, G., Klumperman, J., and Clague, M. J. (2003). The UIM domain of Hrs couples receptor sorting to vesicle formation. *J. Cell Sci.* 116, 4169–4179.
- van Deurs, B., Holm, P. K., Kayser, L., and Sandvig, K. (1995). Delivery to lysosomes in the human carcinoma cell line HEp-2 involves an actin filament-facilitated fusion between mature endosomes and preexisting lysosomes. *Eur. J. Cell Biol.* 66, 309–323.
- VerPlank, L., Bouamr, F., LaGrassa, T. J., Agresta, B., Kikonyogo, A., Leis, J., and Carter, C. A. (2001). Tsg101, a homologue of ubiquitin-conjugating (E2) enzymes, binds the L domain in HIV type 1 Pr55(Gag). *Proc. Natl. Acad. Sci. USA* 98, 7724–7729.
- White, I. J., Bailey, L. M., Razi Aghakhani, M., Moss, S. E., and Futter, C. E. (2006). EGF stimulates annexin 1-dependent inward vesiculation in a multivesicular endosome subpopulation. *EMBO J.* 25, 1–12.
- Yamashiro, D. J., Tycko, B., Fluss, S. R., and Maxfield, F. R. (1984). Segregation of transferrin to a mildly acidic (pH 6.5) para-Golgi compartment in the recycling pathway. *Cell* 37, 789–800.
- Yan, Q., Sun, W., Kujala, P., Lotfi, Y., Vida, T. A., and Bean, A. J. (2005). CART: an Hrs/actinin-4/BERP/myosin V protein complex required for efficient receptor recycling. *Mol. Biol. Cell* 16, 2470–2482.